Catalysis Letters 62 (1999) 131–138

A comparison of the NO–CO reaction over Rh(100), Rh(110) and Rh(111)

G.S. Herman [a,*], C.H.F. Peden [a], S.J. Schmieg [b,**] and D.N. Belton [b,***]

[a] *Environmental Molecular Science Laboratory, Pacific Northwest National Laboratory, PO Box 999, MSIN K8-93, Richland, WA 99352, USA*
E-mail: gs.herman@pnl.gov

[b] *Physical Chemistry Department, General Motors Research and Development Center, 30500 Mound Road, Warren, MI 48090-9055, USA*

Received 9 June 1999; accepted 23 July 1999

Reaction rates and product selectivities were measured over the Rh(100) surface as a function of temperature, and CO and NO partial pressures. These results are compared with our prior studies of the NO–CO reaction on the Rh(111) and Rh(110) surfaces. The only products detected for all three surfaces were CO_2, N_2O, and N_2. Furthermore, for the Rh(100) surface we have found a significant change in the apparent activation energy (E_a) with reaction temperature. For the Rh(100) surface it was found that the E_a can change by a factor of 2.3 in the temperature range investigated here, from 528 to 700 K, with the lower values obtained at higher temperatures. In contrast, E_a's were found to remain constant over the same temperature range for the Rh(110) and Rh(111) surfaces. The results observed for the Rh(100) surface suggest that reaction kinetics are dominated by variations in NO coverages. At low temperatures, the surface is fully saturated with NO, and dissociation is limited by the availability of vacancy sites through NO desorption. At high temperatures, the surface is still primarily covered with NO, however, the number of vacancy sites has increased substantially. In this case, we propose that the apparent activation energy is now reflecting NO dissociation kinetics rather than those for NO desorption.

Keywords: NO–CO reaction, rhodium, NO_x reduction, structure sensitive reaction

1. Introduction

The interaction of NO with rhodium surfaces has been extensively studied because of rhodium's uniquely high activity for reduction of nitrogen oxides (NO_x) in automotive three-way catalysts [1,2]. In addition to its high activity for NO_x reduction, Rh is effective for CO oxidation and shows good resistance to thermal degradation. The analysis of kinetic data from single-crystal surfaces has provided significant insight into the mechanism by which mixtures of NO, CO, and O_2 reactions proceed [3–9]. Single-crystal surfaces have the advantage that they are well defined in terms of structure and composition and, furthermore, the rates of individual steps can be measured. It is the combination of individual step kinetics with overall reaction rates that ultimately validate a proposed reaction mechanism [3].

Recently, an extensive study was performed to measure the structure sensitive selectivity of the NO–CO reaction over Rh(110) and Rh(111) surfaces [4]. Kinetic measurements of the NO conversion rate indicated that reaction over the Rh(110) surface is between 1.3 and 6.3 times faster than that over the Rh(111) surface over the ranges of temperature (528–670 K), total pressures (48 Torr), and CO/NO ratios (0.125–8) studied. Also, it was found that Rh(110) was considerably more selective for the formation of N_2 vs. N_2O than the Rh(111) surface under all the conditions studied. The higher selectivity towards N_2 was attributed to more facile dissociation of NO on the more open structure of the (110) surface. The N atoms that resulted from NO dissociation can react with either NO or N to form N_2O or N_2, respectively. Likewise, the adsorbed oxygen generated by NO dissociation reacts with CO to form CO_2. This model is consistent with the selectivities observed for both the Rh(110) and Rh(111) surfaces.

The current study is an extension of our previous work [4]. We have performed kinetic measurements for the Rh(100) surface under identical conditions as those previously reported for Rh(110) and Rh(111). We have found that the NO conversion rate for the Rh(100) surface is comparable to that measured for the Rh(110) and Rh(111) surfaces. We have also found that the selectivity for the formation of N_2 is intermediate between the Rh(110) and Rh(111) surfaces. These results are consistent with our model in which the activity and selectivity depend on the density of rhodium atoms in the top-most layer. (The corresponding surface atomic densities for these three surfaces are in the order Rh(111) $>$ Rh(100) $>$ Rh(110).) In our model, the activity and selectivity are dominated by steric hindrance of the NO dissociation elementary step. Thus, the more open surfaces run the reaction faster (at the high NO coverages of this study) and are, thus, more selective for N_2 because of higher N atom coverages.

A prior investigation under identical experimental conditions for the NO–CO reaction on Rh(100) failed to measure the formation of N_2O and, therefore, the authors did

* To whom correspondence should be addressed.
** Current address: General Motors R&D Center, MC 480-106-185, 30500 Mound Road, Warren, MI 48090-9055, USA.
*** Current address: General Motors Powertrain, 3300 GM Rd, MC 483-302-137, Milford, MI 48380, USA.

not consider an important mechanistic step in this reaction [5]. For Rh(111) and Rh(110) (as well as Rh(100) to be shown below), the N_2O reaction channel is an important pathway and, at temperatures below 650 K, this species is found to be the dominant nitrogen-containing product [4]. A second study of the NO–CO reaction on Rh(100) has been reported [6]. In this second study the NO and CO partial pressures were extended over a very wide range, however, there is little overlap in the pressure regime investigated for either of these two studies [5,6]. Hendershot and Hansen [6] reported that only CO_2 and N_2 were detected as reaction products under their experimental conditions. We will discuss in further detail below the importance of including the N_2O reaction channel to fully understand the mechanism of the NO–CO reaction on rhodium surfaces.

2. Experimental

The experiments were performed in a custom built system that combines an UHV analysis chamber connected to a high-pressure (<760 Torr) reactor. The UHV analysis chamber is equipped with several surface analytical techniques. For this study we used X-ray photoelectron spectroscopy (XPS), Auger electron spectroscopy (AES), and low-energy electron diffraction (LEED). The reactor is also connected to a gas manifold, a gas chromatograph (GC), and a turbomolecular pump. The reactor has a volume of 0.438 l and a baratron gauge measures the gas pressures. The gases used in these experiments were NO (99.0%) and CO (99.99%) obtained from Matheson Gas Products. The CO was trapped with a liquid-nitrogen bath to exclude any metal carbonyls from the reactor.

The sample was mounted to a retractable transfer rod that can be moved between the reactor and analysis chamber when both are under UHV conditions. The Rh(100) sample was a disk measuring 0.560 cm in diameter and 0.07 cm thick. Both sides of the sample were oriented to within 1° of the (100) crystal plane. The sample had both sides polished with successively finer grades of diamond paste before a final chemical etch of hot HF/HNO_3 (3 : 1) for several minutes. The sample was mounted to the transfer rod by two high-purity tantalum leads spot-welded to the sides of the crystal for resistive heating. A W/Re (type C) thermocouple was spot-welded to the side of the sample for temperature measurements. The surface area was calculated to be 0.246 cm^2/side and the total number of active sites was calculated to be 6.85×10^{14} (both sides included).

Initially, the sample was placed in the reactor and treated in an 8 Torr CO/8 Torr O_2 gas mixture at 550 K for several cycles. The sample was then transferred to the UHV chamber and both sides of the sample were cleaned and ordered by cycles of Ar^+ sputtering (1 keV, 60 min), annealing at 1325 K (30 min in UHV), and flashing to 1450 K (1 min in UHV). Many cycles of this procedure were required to obtain sharp (1 × 1) LEED patterns. The surface had no contamination as determined by AES and XPS after these procedures.

The experimental procedure for making a rate measurement was as follows: (1) the reactor was evacuated, (2) the NO and CO were leaked into the gas manifold and allowed to mix, (3) the mixture was then leaked into the reactor to the desired pressure and the valve was then closed, (4) the sample was heated to the reaction temperature at a rate of 15 K/s and held at this temperature for a specified time (⩾15 s) while keeping the overall NO conversion below 15%, (5) the sample was then cooled down and the reactant and product gases were allowed to equilibrate for 10 min, (6) the gas mixture was leaked into the evacuated GC sampling line and allowed to mix further; (7) the gases were then injected into the GC.

3. Results

The turnover numbers (TON) for CO_2, N_2O, and N_2 formation on Rh(100) are shown in figure 1 for the reaction of 8 Torr of NO and 8 Torr of CO. The data in figure 1 are plotted in an Arrhenius fashion as a function of inverse temperature. For all three reaction products there is a significant break in the linear behavior at $\sim 1.7 \times 10^{-3}$ K^{-1} ($\sim$590 K) indicative of a change in the apparent activation energy (E_a). The regions above and below this value of inverse temperature will be termed the high-temperature (HT) and low-temperature (LT) regions, respectively. The values of E_a in the HT region are 22.2, 15.3, and 26.2 kcal/mol for CO_2, N_2O, and N_2, respectively. Likewise, the values

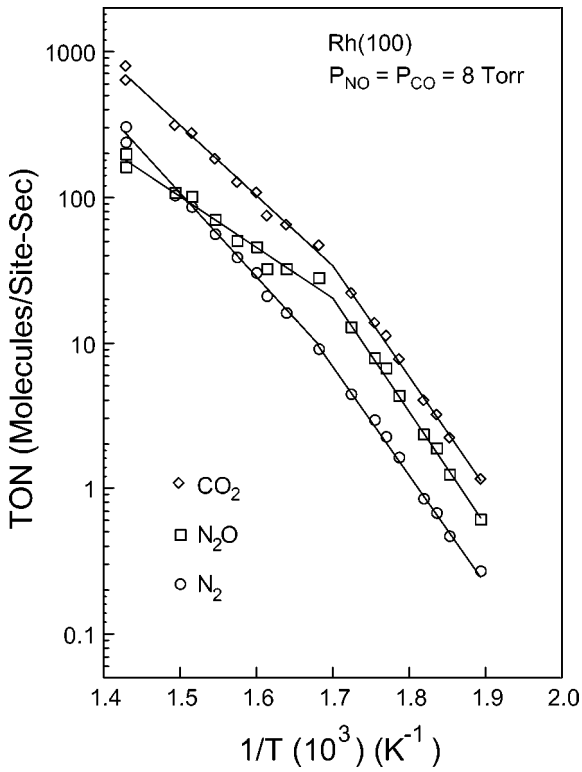

Figure 1. Turnover numbers (TON) for CO_2, N_2O, and N_2 formation for the NO–CO reaction over Rh(100) as a function of inverse temperature. $P_{CO} = P_{NO} = 8$ Torr.

Table 1
Apparent activation energies and frequency factors for CO_2, N_2O, and N_2 formation, and NO loss for the NO–CO reaction over Rh(100), Rh(110), and Rh(111) single-crystal catalysts.[a]

	Rh(100)				Rh(110)[b]		Rh(111)[b]	
	LT		HT					
	E_a	n	E_a	n	E_a	n	E_a	n
CO_2	35.0	3.4×10^{14}	22.2	6.1×10^{9}	28.0	7.3×10^{11}	34.2	5.0×10^{13}
N_2O	35.8	4.2×10^{14}	15.3	1.0×10^{7}	25.3	3.1×10^{10}	35.7	1.1×10^{14}
N_2	33.8	2.6×10^{13}	26.2	4.1×10^{10}	29.6	8.3×10^{11}	32.1	1.6×10^{12}
NO	35.3	7.1×10^{14}	20.5	2.1×10^{9}	27.2	5.6×10^{11}	34.8	1.4×10^{14}

[a] $P_{NO} = P_{CO} = 8$ Torr; E_a (kcal/mol); n (molecules/site s).
[b] From [4].

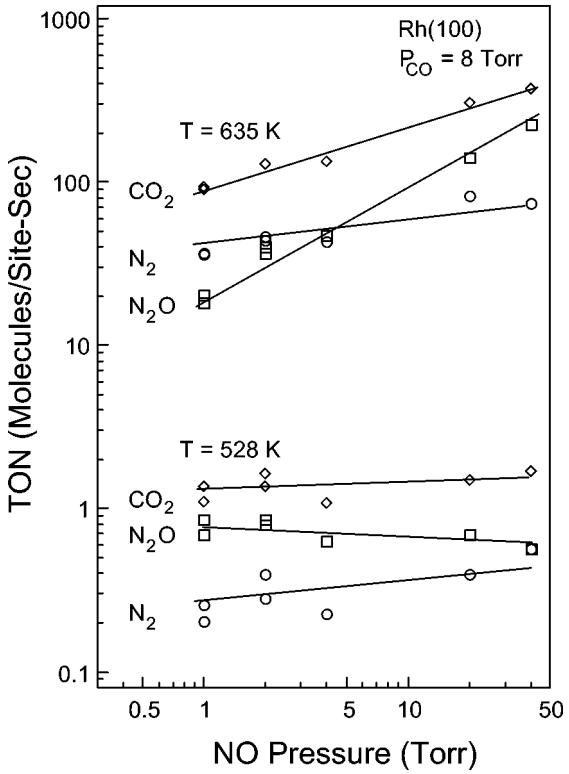

Figure 2. Turnover numbers (TON) for CO_2, N_2O, and N_2 formation for the NO–CO reaction over Rh(100) as a function of NO partial pressure at 528 and 635 K. $P_{CO} = 8$ Torr.

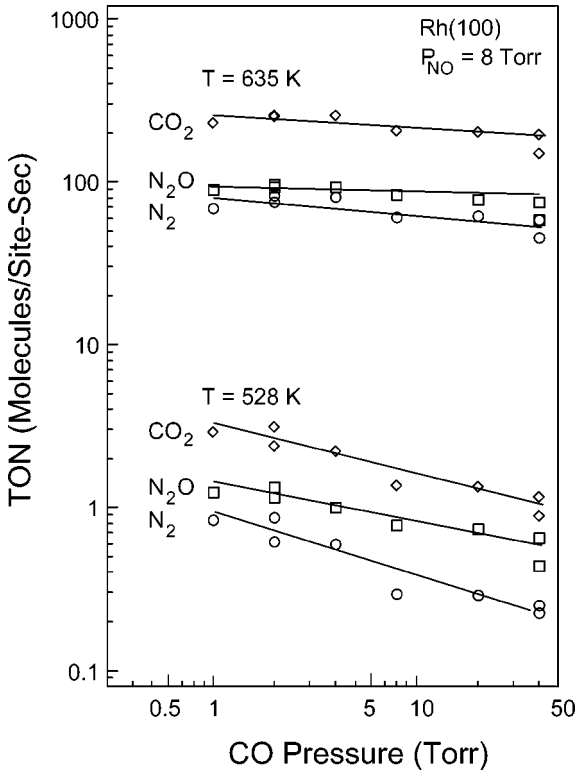

Figure 3. Turnover numbers (TON) for CO_2, N_2O, and N_2 formation for the NO–CO reaction over Rh(100) as a function of CO partial pressure at 528 and 635 K. $P_{NO} = 8$ Torr.

of E_a in the LT region are 35.0, 35.8, and 33.8 kcal/mol for CO_2, N_2O, and N_2, respectively. These values of E_a are summarized in table 1. To determine if the breakpoint observed in the Arrhenius plot for the NO–CO reaction is due to our experimental methods we have also performed the CO–O_2 reaction on Rh(100). In this case we found no breakpoint and an E_a of 27.5 kcal/mol, which is nearly identical to the results observed in the prior study [5], no breakpoint and an E_a of 25.4 kcal/mol. After comparing the results from several runs we estimate the error of our values of E_a to be ± 2 kcal/mol.

Figure 2 shows the effect of NO partial pressure on product formation rates at two reaction temperatures (528 and 635 K). For the experiment in which the figure 2 data were generated, CO pressure was held constant at 8 Torr and NO pressure was varied between 1 and 40 Torr. The 528 and 635 K temperatures correspond to the LT and HT regime as indicated in figure 1, respectively. For the reaction at 528 K, the reaction rate for CO_2, N_2O, and N_2 formation was nearly constant and thus zero order with respect to NO pressure. When the reaction was carried out at 635 K, the N_2 formation rate was zero order in NO pressure, but both CO_2 and N_2O formation rates exhibited positive order NO pressure dependencies of 0.38 and 0.64, respectively.

The effect of CO partial pressures (1–40 Torr) on the TON is illustrated in figure 3 for reactions at both 528 and 635 K for a constant NO pressure of 8 Torr. The 528 and 635 K temperatures again correspond to the LT and HT regime, as indicated in figure 1, respectively. For both the 528 and 635 K data, the reaction rate for CO_2, N_2O, and N_2 formation was approximately constant and thus nearly

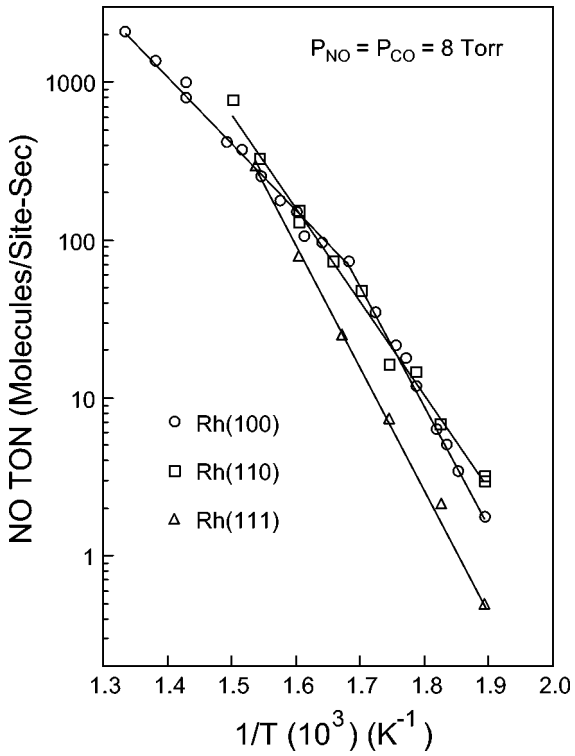

Figure 4. Turnover numbers (TON) for NO consumption for the NO–CO reaction over Rh(100), Rh(110), and Rh(111) as a function of inverse temperature. $P_{CO} = P_{NO} = 8$ Torr. Rh(110) and Rh(111) results from [4].

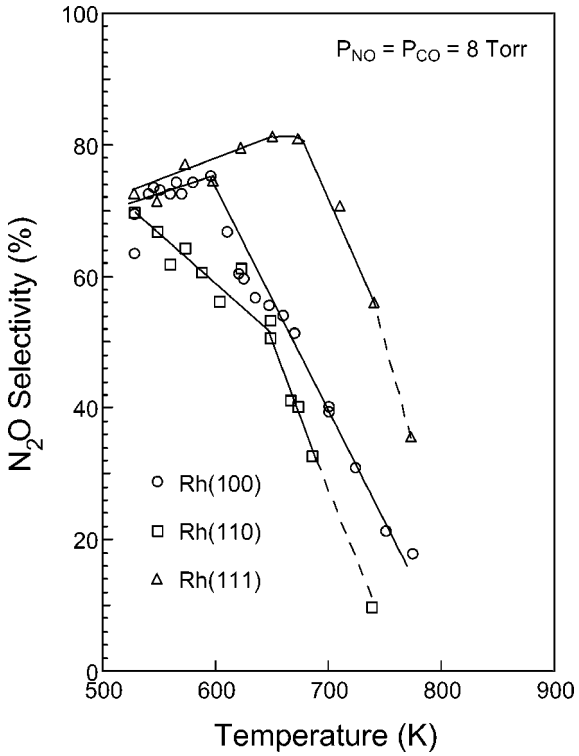

Figure 5. N_2O selectivities for the NO–CO reaction over Rh(100), Rh(110), and Rh(111) as a function of temperature. $P_{CO} = P_{NO} = 8$ Torr. Rh(110) and Rh(111) results from [4].

zero order with respect to CO pressure. At 528 K the N_2O selectivity increases slightly from 60 to 73% in the CO pressure range from 1 to 40 Torr. At 635 K the N_2O selectivity remains constant at a value of 55% in the CO pressure range from 1 to 40 Torr.

A direct comparison of the NO consumption rate over the Rh(100) surface to that over Rh(111) and Rh(110) surfaces is given in figure 4 for a reaction of 8 Torr of NO with 8 Torr of CO. Data for the Rh(111) and Rh(110) surfaces are from a previously published paper [4]. As has been mentioned previously, NO consumption represents the best relative measure of overall activity since it does not depend on the selectivity of the reaction [4]. In this comparison, the NO consumption was calculated based on the TONs obtained for N_2O and N_2 and the stoichiometry of the reaction. This method was used due to the difficulty in measuring small changes in the NO signal from the GC measurement since the total NO consumption was always kept below 15%. Before comparing the TONs it should be noted that the normalized rates for the Rh(110) surface includes sites in both the rows and troughs on this corrugated surface. The Rh(100) and Rh(111) TONs are normalized to only sites in the topmost surface layer. The Rh(111) and Rh(110) data can be described by a single straight line with E_a values of 34.8 and 27.2 kcal/mol, respectively [4]. The Rh(100) data has a LT and HT region, as illustrated before for the reaction products, with E_a values of 35.3 and 20.5 kcal/mol, respectively. These values of E_a are summarized in table 1.

In figure 5 the temperature sensitivity of the N_2O selectivity for NO–CO reaction over the Rh(100) surface is compared to previously published data from Rh(111) and Rh(110) surfaces [4]. For the data in figure 5, the N_2O selectivity is defined as $S_{N_2O} = 100 \times$ [moles N_2O/(moles N_2O + moles N_2)]. For the Rh(100) surface the N_2O selectivity remains approximately constant at 80% for reaction temperatures between 500 and 600 K and decreases linearly from 80% down to 22% between 600 and 800 K. For the Rh(110) surface the N_2O selectivity decreases over the entire temperature range studied; however, the rate of change with temperature is considerably higher above 650 K than below 650 K. Conversely, for the Rh(111) surface the N_2O selectivity increases from 72 to 80% in the temperature range from 500 to 670 K, and then decreases from 80% down to 36% between 670 and 800 K. The dashed lines for the Rh(111) and Rh(110) surfaces are included to indicate that the reaction rates were too fast to accurately measure for these two high-temperature points. For these points, the production of heat from the exothermic reaction leads to instability in the control of the temperature and thus an inaccurate measure of the time at reaction temperature; however, the selectivity of the reaction can be accurately measured in this experiment. In contrast, the Rh(100) did not exhibit this "heat-transfer" limited reaction condition.

Figure 6 shows post-reaction XPS of the three different surfaces. The results for the Rh(111) and Rh(110) surfaces are from our earlier study [4]. For this experiment the NO–CO reaction was run at 528 K with partial pres-

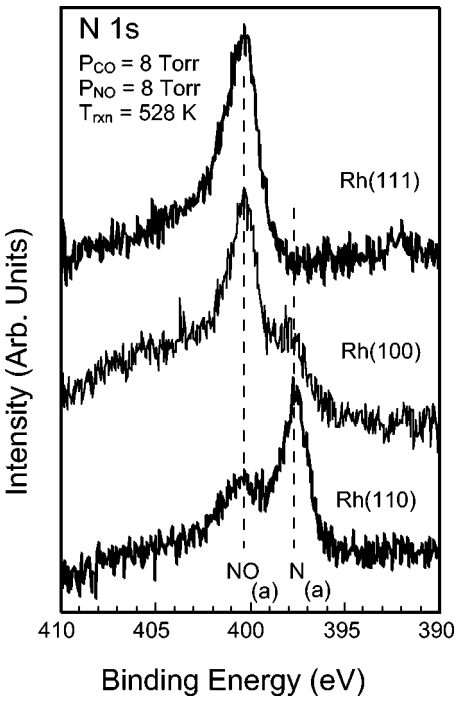

Figure 6. Post-reaction N 1s X-ray photoelectron spectroscopy results for the NO–CO reaction at 528 K over Rh(100), Rh(110), and Rh(111). $P_{CO} = P_{NO} = 8$ Torr. Rh(110) and Rh(111) results from [4].

sures of NO and CO of 8 Torr each. After the reaction, the samples were quenched in the reaction mixture, which was then evacuated before transferring the sample to take the XPS data. The two N 1s spectral features, at binding energies of 397.6 and 400.3 eV, have been assigned to adsorbed N atoms and NO, respectively, as indicated in figure 6. It is clear that the three different surfaces have different relative concentrations of N(ad) and NO(ad) subsequent to steady-state reaction, based on the results of figure 6. The Rh(111) surface consists of only NO(ad), while the Rh(100) and Rh(110) surfaces contain both NO(ad) and N(ad) albeit with differing relative concentrations. The relative intensity of the N(ad) feature increases with decreasing rhodium surface atomic density (surface atomic density: Rh(111) > Rh(100) > Rh(110)).

4. Discussion

We had two goals for the research reported in this paper. First, we wished to address some inconsistencies in the literature about the reaction products and kinetics over the Rh(100) surface. And second, we wanted to challenge our understanding of the NO–CO reaction mechanism to determine if the (100) surface kinetics were consistent with our picture of how surface structure influences reaction kinetics. With regards to reaction kinetics, previously it was reported that the NO–CO reaction over Rh(100), under the identical reaction conditions used here, gave an E_a of 24 kcal/mol for CO_2 formation without the breakpoint in the Arrhenius plot as observed here [5]. Additionally, the previous paper did not report the formation of N_2O, which we now know to be a commonly observed product over all Rh-based catalysts [1,2,4,7–10]. Based on our findings here, we conclude that the (100) surface behaves similar to other Rh-based catalysts in its selectivity towards N_2O. Figure 5 shows the selectivity of three Rh single-crystal surfaces. All three show the same basic trend, that being, high selectivity for N_2O at low temperature with a switch to the formation of predominantly N_2 at higher temperatures. Clearly there is sensitivity in the details of the selectivity vs. temperature profiles to surface structure, a point which we come back to later in the paper. Thus, N_2O is the major N-containing product at low to moderate temperatures over Rh(100) as is true for Rh(111) and Rh(110). However, this is still in apparent contradiction to a second investigation of the NO–CO reaction on Rh(100), in which no N_2O was observed [6]. In the experiments of Hendershot and Hansen [6] much lower partial pressures of NO and CO were used compared to this study. For example, the temperature dependence of the reaction rate was performed with CO and NO partial pressures of 0.06 and 0.43 Torr, respectively. Thus, the lack of N_2O as a reaction product in the data of Hendershot and Hansen [6] is likely due to the reaction conditions investigated. The majority of the experiments were performed at high temperatures (688 K) and low NO partial pressures (0.43 Torr). Both of these factors are likely to result in higher selectivities for the production of N_2. It is well known that going to much lower NO partial pressures can significantly alter the apparent activation energies and the selectivities of the reaction [7]. For example, the N_2O selectivity for Rh(111) was found to decrease more quickly at lower temperatures (e.g., $\sim$150 K lower in temperature than the results shown in figure 5) when the NO and CO partial pressures were reduced by a factor of 10 and 2, respectively. Furthermore, a striking feature of the Hendershot and Hansen results is that a change in the E_a was observed at virtually the same temperature as in our study.

The reaction rates and N_2O selectivities for the Rh(100) surface were found to be sensitive to NO partial pressure at 635 K, and were essentially zero order in NO partial pressure at 528 K. At 635 K, both CO_2 and N_2O formation rates exhibited positive order NO pressure dependence, while the N_2 formation rates were zero order. These results are essentially identical to those previously reported for Rh(111) and Rh(110) surfaces for temperatures below 600 K [4,8]. However, at temperatures above 600 K all three surfaces vary considerably. For example, for the Rh(111) surface at 623 K the formation rates for N_2, CO_2, and N_2O were found to be slightly negative order in NO partial pressure [4]. The lack of sensitivity for the Rh(111) surface can be explained by a mechanism in which the NO and N atom concentrations at the surface do not change with changes in NO partial pressure. Based on post-reaction XPS measurements, the N atom concentration on the Rh(111) surface is known to be very low (e.g., figure 6), suggesting a surface that is fully saturated with NO even down to NO partial pressures

of 1 Torr at 623 K. Furthermore, for the Rh(110) surface at 623 K the formation rates for CO_2 and N_2O were found to be slightly negative order (and slightly positive order for N_2) for NO partial pressures between 1 and 8 Torr, and nearly zero order for higher NO partial pressures [4]. It was suggested that the change in the formation rates observed for the Rh(110) surface at low NO partial pressures and high temperatures (>600 K) was related to changes in the NO surface coverage. For example, with decreasing NO partial pressure the CO_2 formation increased and the N_2O selectivity decreased. The increase in CO_2 formation at low NO partial pressures (i.e., low NO surface coverages) can be rationalized by a model in which the NO dissociation rate limits the overall reaction rate, and that this rate is lower at higher NO surface coverages [4]. The observed decrease in N_2O selectivity at low NO partial pressures (i.e., low NO surface coverages) can be understood by a mechanism in which the relative coverage of N atoms to NO at the surface increases leading to a correspondingly higher propensity for N_2 formation relative to N_2O.

For the Rh(100) surface at 635 K the N_2O selectivity and CO_2 formation rates are found to increase with increasing NO partial pressure. These results can be explained by a mechanism in which the NO surface coverage increases with increasing NO partial pressure, and the surface is not fully saturated with NO even for $P_{NO} = 40$ Torr at 635 K. As for the Rh(110) surface, the observed decrease in N_2O selectivity at low NO partial pressures (i.e., low NO surface coverages) can be understood by a mechanism in which the relative coverage of N atoms to NO at the surface increases leading to a correspondingly higher propensity for N_2 formation relative to N_2O. However, unlike the Rh(110) surface, there is an increase in CO_2 formation with increasing NO partial pressures (i.e., higher NO surface coverages) for Rh(100). The CO_2 formation rate can be used as a measure of the NO dissociation rate due to the relatively fast rate of the reaction between CO and adsorbed O. The steady increase in CO_2 formation of Rh(100) with increasing NO partial pressure indicates that the surface is not fully saturated with NO, and, hence, not limiting dissociation of NO. Similar results were observed for the Rh(111) surface at 598 K at lower NO and CO pressures (below 1 and 4 Torr, respectively) which were explained via a similar mechanism [11].

The most striking feature observed in figures 1 and 4 are the break points in the kinetic data for the Rh(100) surface, but not for the Rh(111) or Rh(110) surfaces. Furthermore, the breakpoint was not observed in a prior study of Rh(100) under identical conditions [5]. Several different experimental methodologies were performed to try and determine if this breakpoint for the Rh(100) was an experimental artifact. These methodologies included varying the order in which the data was obtained, cleaning the sample after each reaction, and not cleaning the sample after each reaction. After each series the breakpoint remained and the location and calculated E_a values were consistent. This leads us to believe that the data presented here are representative of this reaction under these conditions, and benefit from having the reactions run at sixteen different temperatures compared to nine as in the previous study [5]. The higher number of data points in this study may make the breakpoint easier to observe. It is difficult to assign this break in apparent activation energy to any individual reaction step based on this data alone. However, we will discuss some possibilities based on a combination of the results.

The second point we address in this paper is how these data from the (100) surface fit with our understanding of the overall NO–CO reaction mechanism on Rh surfaces. To better understand the effect of surface structure on reaction kinetics it is useful to first discuss the reaction mechanism that we favor for the NO–CO reaction; a mechanism which we take to be the simplest of the proposed NO–CO reaction mechanisms [3]. The reaction can be broken down into six elementary steps where S represents a site for adsorption on the surface:

$$\mathrm{CO(g)} + \mathrm{S} \rightleftharpoons \mathrm{CO(ad)} \quad (1)$$

$$\mathrm{NO(g)} + \mathrm{S} \rightleftharpoons \mathrm{NO(ad)} \quad (2)$$

$$\mathrm{NO(ad)} + \mathrm{S} \rightarrow \mathrm{N(ad)} + \mathrm{O(ad)} \quad (3)$$

$$\mathrm{CO(ad)} + \mathrm{O(ad)} \rightarrow \mathrm{CO_2(g)} + 2\mathrm{S} \quad (4)$$

$$\mathrm{NO(ad)} + \mathrm{N(ad)} \rightarrow \mathrm{N_2O(g)} + 2\mathrm{S} \quad (5)$$

$$\mathrm{N(ad)} + \mathrm{N(ad)} \rightarrow \mathrm{N_2(g)} + 2\mathrm{S} \quad (6)$$

The adsorption or dissociation of the reactants is intimately related to the availability of sites at the surface (i.e., reactions (1)–(3)). In this model, the relative rates of reactions (5) and (6) dictate the relative N_2O selectivity, and are the only two pathways for the removal of N(ad) from the surface. Reactions (5) and (6) are dependent on the relative surface coverages of NO and N. The only available source of N(ad) is from reaction (3), which is dependent on both the presence of NO(ad) and binding sites. The formation of CO_2 (reaction (4)) requires the presence of O(ad) from reaction (3) and CO(ad) from reaction (1). Modeling [1] and FTIR [11] studies for Rh(111) surfaces at moderate NO and CO pressures (8 Torr) have indicated that, at temperatures below ~650 K, the surface is predominately covered by adsorbed NO. Above 650 K the amount of NO on the surface is reduced, and modeling indicates that the relative concentration of N(ad) and open surface sites increase substantially. Although these calculations and measurements have not been carried out for either the Rh(100) or Rh(110) surfaces some generalizations related to the rate-limiting steps may be obtained.

In our prior study we proposed that the differences observed between the activity towards NO consumption for the Rh(111) and Rh(110) surfaces is related to the manner in which adsorbed NO inhibits the dissociation reaction [4]. NO turnover numbers for Rh(100) are found to be between those for the Rh(111) and Rh(110) surfaces over a wide temperature range, as shown in figure 4. Therefore, the

activity of the NO–CO reaction (Rh(110) > Rh(100) > Rh(111)) is inversely related to the surface atomic density in the top layer (Rh(110) < Rh(100) < Rh(111)). At low temperatures (∼528 K) and moderate NO and CO pressures (∼8 Torr), the three different surfaces do have increasing concentrations of adsorbed N relative to NO based on post-reaction XPS (e.g., figure 6), further demonstrating the relationship of the surface atomic density in the top layer (Rh(110) < Rh(100) < Rh(111)) to NO dissociation rates. Thus, the results that were obtained for the Rh(100) surface are fully consistent with our prior model in which adsorbed NO inhibits the NO dissociation reaction and the overall NO consumption kinetics at low temperatures and moderate pressures.

To understand the origin of the change in the E_a for the reaction products on the Rh(100) surface, we compare to other studies that have observed a similar change in their data. For polycrystalline films of Rh, a similar break, at $\sim 1.7 \times 10^{-3}$ K^{-1}, in the Arrhenius plot for the NO–CO reaction has been observed [12]. Surface-enhanced Raman spectroscopy (SERS) was used in this study and it was observed that a vibrational feature at 315 cm^{-1}, assigned to the Rh–N stretch of N(ad), is significantly reduced in intensity in the temperature range of 573–623 K (i.e., where the break occurs) [12]. The authors suggested that the reduction of N(ad) at the surface at higher temperatures results in a change in the apparent activation energy. The difference in the probable surface structure and reaction conditions between these two studies makes direct comparison difficult. However, the similarity between these two different studies suggest that the concentration of N(ad) may have a strong impact on the NO–CO reaction at low temperatures. Likewise, it has been noted that N_2 formation from N(ad) recombination occurs at higher temperatures on the Rh(100) surface (770 K), compared with the Rh(111) (660 K) and Rh(110) (580 K) surfaces [5]. These differences may have implications that are related to the change in E_a for Rh(100).

To investigate the effect of temperature on the concentration of N(ad), we performed post-reaction XPS, shown in figure 7, for the Rh(100) surface after reaction at 528, 635, and 700 K. The 528 K value corresponds to a reaction in the LT regime as defined earlier, and the 635 and 700 K values correspond to reactions in the HT regime. Note that this data is obtained after the Rh crystal has rapidly cooled in the reaction mixture. Thus, we do not believe the relative NO(ad) concentrations under reaction conditions are accurately reflected in these data. It is clear from this data that as the reaction temperature increases, the relative intensity of the N(ad) component in the post-reaction XPS is reduced. These data appear to suggest that the concentration of N(ad) may be related to the changes observed in the apparent activation energies that were determined from figure 1. We rationalize these results in the following way. As discussed above, the LT regime on Rh(100) displays reaction kinetics that suggest a reaction limited by NO desorption (reverse of reaction (2)). In this case, the

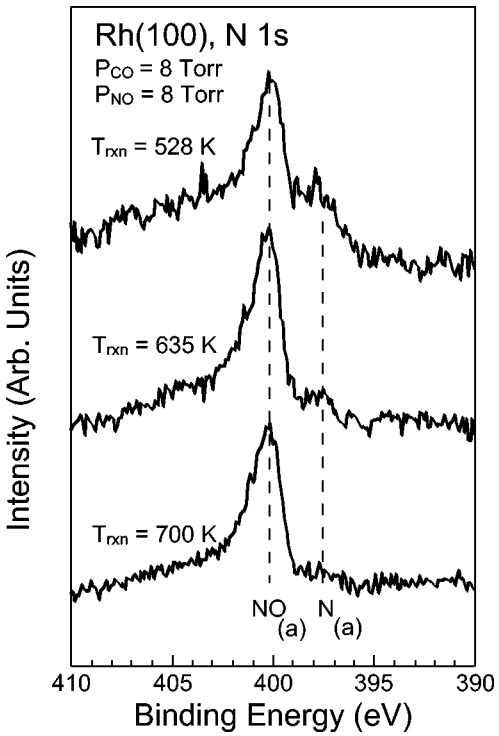

Figure 7. Post-reaction N 1s X-ray photoelectron spectroscopy results for the NO–CO reaction over Rh(100) obtained after reaction at 528, 635, and 700 K. $P_{CO} = P_{NO} = 8$ Torr.

availability of vacant sites needed for NO dissociation (reaction (3)) is low due to the high concentrations of both NO(ad) and N(ad). At higher temperatures, concentrations of both of these adsorbed species are reduced substantially so that the availability of vacant sites is no longer an issue. Therefore, in the HT regime it may well be that NO dissociation rather than NO desorption is rate limiting. In turn, this could be because the concentration of NO(ad) is low. It is interesting to note that the N_2O selectivity in the LT region (figure 5) is nearly constant, and once the sample reaches the HT region the selectivity rapidly decreases. Also note that the selectivity for N_2O increases with increasing NO pressures in the HT regime (figure 2). These changes in selectivity and kinetics are again an indication of considerable changes in NO(ad) coverages between the LT and HT regime.

5. Conclusions

The consumption of NO indicates that the activity of the Rh(100) surface lies between the Rh(110) and Rh(111) surfaces, where the Rh(110) surface is the most active. The NO consumption data fits well with our prior model that the rate-limiting step in the NO–CO reaction on Rh is the dissociation of NO, and that this step is hindered at low temperatures by steric effects on the more closely packed surfaces. Selectivities to N_2O production indicate that the selectivity of the Rh(100) surface lies between those of the Rh(110) and Rh(111) surfaces, where Rh(111) has the high-

est selectivity to N_2O production in the temperature range investigated. It has been found here that the NO–CO reaction on the Rh(100) surface behaves differently than the Rh(110) and Rh(111) surfaces in some interesting aspects. The primary difference is that the apparent activation energy for the reaction products has a breakpoint at 590 K, and can be split into high- and low-temperature components. The breakpoint in the apparent activation energy for the Rh(100) surface appears to be related to an increased concentration of adsorbed N(ad) and NO(ad) on the surface at low temperatures, and dissociation is limited by the availability of adsorption sites through NO desorption. At higher temperatures both the N(ad) and NO(ad) concentrations are significantly reduced leading to an apparent activation energy that is dominated by NO dissociation.

Acknowledgement

Pacific Northwest National Laboratory (PNNL) is operated for the US Department of Energy (DOE) by Battelle Memorial Institute under Contract No. DE-AC06-76RLO 1830. This work was supported primarily by the US DOE, Office of Basic Energy Sciences, Division of Chemical Sciences, and in part by the DOE Office of Health and Environmental Research through the Environmental Molecular Sciences Laboratory project at PNNL.

References

[1] V.P. Zhdanov and B. Kasemo, Surf. Sci. Rep. 29 (1997) 31, and references therein.
[2] K.C. Taylor, Catal. Rev. Sci. Eng. 35 (1993) 457, and references therein.
[3] D.N. Belton, C.L. DiMaggio, S.J. Schmeig and K.Y.S. Ng, J. Catal. 157 (1995) 59.
[4] C.H.F. Peden, D.N. Belton and S.J. Schmieg, J. Catal. 155 (1995) 204.
[5] C.H.F. Peden, D.W. Goodman, D.S. Blair, P.J. Berlowitz, G.B. Fisher and S.H. Oh, J. Phys. Chem. 92 (1988) 1563.
[6] R.E. Hendershot and R.S. Hansen, J. Catal. 98 (1986) 150.
[7] H. Permana, K.Y.S. Ng, C.H.F. Peden, S.J. Schmieg, D.K. Lambert and D.N. Belton, J. Catal. 164 (1996) 194.
[8] D.N. Belton and S.J. Schmieg, J. Catal. 144 (1993) 9.
[9] H. Permana, K.Y.S. Ng, C.H.F. Peden, S.J. Schmieg, D.K. Lambert and D.N. Belton, Catal. Lett. 47 (1997) 5.
[10] W.C. Hecker and A.T. Bell, J. Catal. 84 (1983) 200.
[11] H. Permana, K.Y.S. Ng, C.H.F. Peden, S.J. Schmieg and D.N. Belton, J. Phys. Chem. 99 (1995) 16344.
[12] A.T. Tolia, C.T. Williams, C.G. Takoudis and M.J. Weaver, J. Phys. Chem. 99 (1995) 4599.